



Temperature dependence of the energy bandgap of two-dimensional hexagonal boron nitride probed by excitonic photoluminescence

X. Z. Du, C. D. Frye, J. H. Edgar, J. Y. Lin, and H. X. Jiang

Citation: [Journal of Applied Physics](#) **115**, 053503 (2014); doi: 10.1063/1.4863823

View online: <http://dx.doi.org/10.1063/1.4863823>

View Table of Contents: <http://scitation.aip.org/content/aip/journal/jap/115/5?ver=pdfcov>

Published by the [AIP Publishing](#)



Re-register for Table of Content Alerts

Create a profile.



Sign up today!



Temperature dependence of the energy bandgap of two-dimensional hexagonal boron nitride probed by excitonic photoluminescence

X. Z. Du,¹ C. D. Frye,² J. H. Edgar,² J. Y. Lin,¹ and H. X. Jiang^{1,a)}

¹Department of Electrical and Computer Engineering, Texas Tech University, Lubbock, Texas 79409, USA

²Department of Chemical Engineering, Kansas State University, Manhattan, Kansas 66506-5102, USA

(Received 19 November 2013; accepted 20 January 2014; published online 3 February 2014)

Hexagonal boron nitride (hBN) is an emerging material for the exploration of new physics in two-dimensional (2D) systems that are complementary to graphene. Nanotubes with a diameter (~ 60 nm) that is much larger than the exciton binding energy in hBN have been synthesized and utilized to probe the fundamental optical transitions and the temperature dependence of the energy bandgap of the corresponding 2D hBN sheets. An excitonic transition at 5.901 eV and its longitudinal optical phonon replica at 5.735 eV were observed. The excitonic emission line is blue shifted by about 130 meV with respect to that in hBN bulk crystals due to the effects of reduced dimensionality. The temperature evolution of the excitonic emission line measured from 300 to 800 K revealed that the temperature coefficient of the energy bandgap of hBN nanotubes with large diameters (or equivalently hBN sheets) is about 0.43 meV/K, which is a factor of about 5 times smaller than the theoretically predicted value for the transitions between the π and π^* bands in hBN bulk crystals and 6 times smaller than the measured value in AlN epilayers with a comparable energy bandgap. The observed weaker temperature dependence of the bandgap than those in 3D hBN and AlN is a consequence of the effects of reduced dimensionality in layer-structured hBN.

© 2014 AIP Publishing LLC. [<http://dx.doi.org/10.1063/1.4863823>]

I. INTRODUCTION

The synthesis, properties, and device applications of layer-structured hexagonal boron nitride (hBN) have come under intense investigation in recent years. Due to its wide bandgap (~ 6 eV)¹⁻⁴ and high emission efficiency,⁵ hBN has a significant potential for deep ultraviolet (DUV) photonic device applications. Additionally, the high neutron capture cross-section of the isotope boron-10 makes hBN a unique material for neutron detector applications.⁶ Due to its similar in-plane lattice constant to graphene and chemical inertness and resistance to oxidation, hBN is also considered as an ideal material for the exploration of van der Waals heterostructures made layer by layer between hBN/graphene related materials with new physics and applications.^{7,8} A recent theoretical study has also suggested that quasi free-standing silicene can be realized in a superlattice structure with hBN.⁹ Consequently, the full understanding of the optical properties of hBN is necessary for the design and applications of devices based on hBN and its related heterostructures.

While the potentials of hBN for active DUV photonic,¹⁰⁻¹⁴ neutron detector,⁶ and electron emitter¹⁵ device applications are being explored, experimental data on fundamental optical transitions in two-dimensional (2D) hBN sheets and one-dimensional (1D) nanotubes are scarce. The band edge emission spectra of the three-dimensional (3D) hBN bulk crystals are generally known to be dominated by two series of bands; four sharp Frenkel class exciton levels labeled as the S-series bands¹⁶⁻¹⁸ and another relatively broader lines labeled as the D-series bands.^{16,17} A previous optical absorption measurement performed on hBN revealed

a very small temperature coefficient of less than 4×10^{-5} eV/K for the bandgap of hBN.¹⁹ This abnormally low value was explained theoretically by the absence of the two center boron-nitrogen terms in the expression for the gap due to the special symmetry of the p -point in the hexagonal Brillouin zone.¹⁹ At the same time, the theory predicated a much higher temperature coefficient of ~ 2.1 meV/K for the transitions between the π and π^* bands.¹⁹ More recent theoretical works indicated that the selection rules only allow the transitions between the π and π^* bands in hBN.¹⁻³ However, there have not been experimental works performed on the temperature dependence of the excitonic emission peaks in hBN in either 3D, 2D, or 1D form in a large temperature range. This is due partly to the fact that the fine features of the S-series excitonic bands tend to vanish at high temperatures owing to the co-existence of the D-series emission lines.^{16,17} It was speculated that the observation of the S-series excitonic emission bands is associated with a more perfect crystalline structure, while the D-series emission bands may be associated with a crystalline structure that deviates (or deformed) from the perfect stacking sequence.^{12,16} As a result, the temperature dependencies of the band edge transitions and of the bandgap of hBN are not clear so far, despite the fact that these dependencies are fundamentally important for a semiconductor material system in the development stage.

The optical absorption spectra of hBN in 3D, 2D, and 1D forms have been calculated,³ which revealed that the optical properties of hBN nanotubes with diameters exceeding the exciton binding energy in hBN (>10 Å) are the same as those of the 2D hBN sheets. We report here on the synthesizing and variable temperature (10–800 K) photoluminescence (PL) studies of hBN nanotubes with a large diameter of

^{a)}hx.jiang@ttu.edu

~ 60 nm. The low temperature PL spectra of 2D hBN exhibit two dominant emission lines at 5.901 eV and 5.735 eV, which have not been previously observed. Based on the similar decay characteristics, the 5.735 eV emission line can be attributed to the longitudinal optical (LO) phonon replica of the 5.901 eV line. The main peak at 5.901 eV is blue shifted with respect to the lowest exciton level in hBN bulk crystals. It is thus most plausible that the observed main emission peak at 5.901 eV is due to the exciton recombination and the blue shift is associated with effects of reduced dimensionality. From the dependence of the excitonic emission peak measured from 300 K to 800 K, we extract the temperature coefficient (α) of the energy gap of hBN nanotubes with a large diameter (or equivalently hBN sheets) is about $0.43 \text{ meV}/^\circ\text{K}$, which is about 5 times smaller than the theoretically predicted value of $\sim 2.1 \text{ meV}/^\circ\text{K}$ for the transitions between the π and π^* bands in 3D hBN.¹⁹

II. EXPERIMENT

Multi-walled hBN nanotubes were synthesized by chemically etching high purity pyrolytic boron nitride (pBN) in molten alkali salts, resulting in nanotubes densely covering and attached to the pBN surface. At first, high purity pBN, the starting material for the nanotubes formation, was prepared by polishing its surface by hand until it became shiny. Next, the pBN was etched at 425°C in an equimolar mixture of molten sodium hydroxide and potassium hydroxide for 10 min. The sample was then rinsed in water to remove any residual etchant. Scanning electron microscope (SEM) imaging has been performed at a voltage of 5 kV to evaluate the size and morphology of resulting BN nanotubes (Figure 1). The diameter and length of the hBN nanotubes are approximately 60 nm and $5 \mu\text{m}$, respectively. The hBN nanotubes are grown randomly, but mostly within the plane. The diameters of these hBN nanotubes also appear quite uniform. Based on the size of these nanotubes, the measured optical properties will represent those of 2D hBN sheets.³

Bulk crystals of hBN employed in this study were grown at ambient pressure by the flux method using a nickel (Ni)

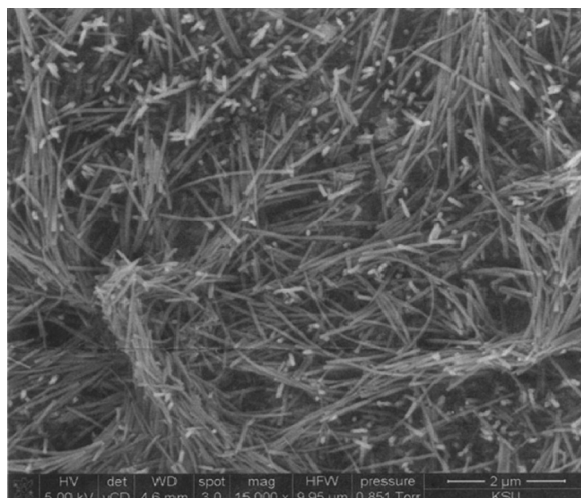


FIG. 1. SEM image of hBN nanotubes sample used in this study. The scale bar on the bottom right corner is for $2 \mu\text{m}$.

and chromium (Cr) solvent mixture. High purity hBN powder and nitrogen gas were used as B and N sources. The source materials were soaked at 1525°C for 6 h and then followed by subsequent cooling at a slow rate of $4^\circ\text{C}/\text{h}$ until solvent solidification. A slow cooling rate was employed to insure the precipitation of high quality crystals. A detailed description of hBN crystal growth was discussed elsewhere.²⁰

For PL measurements, a frequency-quadruped Ti-sapphire laser (with lasing wavelength of 197 nm, 76 MHz repetition rate, 100 fs pulse width, and average optical power of about 1 mW) was used as an excitation source. The laser beam was focused onto the sample surface by a lens. The PL signal was collected and dispersed by a monochromator (1.3 m) and then detected by a microchannel-plate photomultiplier tube together with a single photon-counting system providing a time-resolution of about 20 ps.¹²

III. RESULTS AND DISCUSSION

Figure 2 shows the comparison of PL spectra of 2D hBN nanotubes with a diameter of 60 nm and hBN bulk crystal measured side-by-side at 10 K. The main emission peaks in hBN bulk crystals at 5.772 eV and 5.800 eV were attributed to the Frenkel class free exciton levels.^{1-3,16-18,21} The detailed spectral features exhibited by hBN bulk crystals and hBN nanotubes are quite different. The emission peaks in hBN nanotubes at 5.901 and 5.735 eV have not been previously reported. The peak with the highest emission energy in hBN nanotubes is blue shifted (by $\sim 130 \text{ meV}$) with respect to the emission line of the lowest exciton energy level at 5.772 eV in hBN bulk crystals. Reduced dimensionality effects are believed to account for this blue shift. Decreasing the dimensionality of hBN from 3D to 2D and 1D leads to two competing mechanisms³ that will affect the exciton

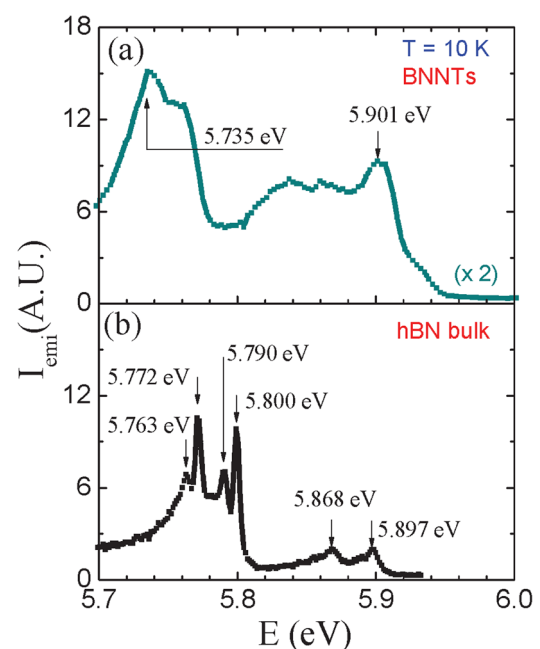


FIG. 2. PL spectra of (a) hBN nanotubes (BNNTs) with a diameter of 60 nm and (b) an hBN bulk crystal measured at $T = 10 \text{ K}$.

transition peak (E_p): (i) the excitonic binding energy tends to increase from 0.7 eV in 3D to 2.1 eV in 2D and 3.0 eV in 1D, which decreases E_p , and (ii) the quasi-particle energy gap will increase by almost the same order of magnitude, which increases E_p . As a result, the position of the first excitonic peak is almost independent of the nanotube radius and system dimensionality.³ However, the calculation results clearly revealed a blue shift by an amount of about 170 meV for the exciton transition in hBN single sheets (or hBN nanotubes with large diameters) with respect to that in hBN bulk crystals. Therefore, the experimentally observed blue shift of 130 meV here appears to be within a reasonable range of deviation from the calculated value of 170 meV.³ We thus assign the 5.901 eV line to the excitonic transition in hBN sheet. Although these emission lines in hBN nanotubes are broader than the exciton emission lines in the bulk crystals, the observation of the excitonic transitions in hBN nanotubes (or sheets) may be an indicative of the realization of hBN nanotubes/sheets with higher crystalline quality and purity than previous attainments.^{22–25} The spectral broadening could be attributed to fact that these nanotubes are multi-walled tubes so that the corresponding 2D hBN sheets are multiple sheets in which the B and N atoms are not necessarily perfectly aligned between the rolled sheets.

Figure 3 shows the PL decay characteristics of the emission lines at 5.901 eV and 5.735 eV in hBN nanotubes measured at $T = 10$ K. The decay kinetics of both lines follows two-exponential decay function

$$I(t) = I_1 \exp\left(-\frac{t}{\tau_1}\right) + I_2 \exp\left(-\frac{t}{\tau_2}\right), \quad (1)$$

where $I(t)$ is the emission intensity at decay time t , τ_1 and τ_2 are the characteristic decay lifetimes of the fast and slow components, respectively, and I_1 and I_2 are the initial peak intensities related to the fast and slow components, respectively, at $t = 0$. The decay characteristics of both emission peaks at 5.901 eV and 5.735 eV exhibit almost identical behaviors: the PL decay process is characterized by two-exponential decay with lifetimes $\tau_1 \sim 0.14$ ns and $\tau_2 \sim 1.2$ ns. This indicates that these two transitions share the same origin. The energy separation between these two emission peaks is 166 meV, which is very close the LO phonon energy of 169 meV in hBN.²⁶ The LO phonon energy in hBN tends to decrease with lowering the dimensions.²⁷ Thus, the 166 meV energy difference between the 5.901 eV and 5.735 eV transition peaks is most probable the energy of the LO phonon in hBN nanotubes with large diameters or sheets. This means that the later is the 1LO phonon replica of the former. The observed similar decay characteristics of these two emission lines further corroborates this assignment.

The temperature evolution of the PL spectra of the hBN nanotubes from 10 K to 800 K is shown in Fig. 4. Each spectrum has been shifted vertically for clarity. The temperature dependent PL energy peak position (E_p), which is at 5.901 eV at 10 K, as well as the related PL intensity have been extracted from the temperature evolution of the spectra and plotted in Figs. 5(a) and 5(b), respectively. The spectral peak positions of the exciton transition, $E_p(T)$, red-shift from 5.901 eV at 10 K to about 5.65 eV at 800 K and the temperature variation follows

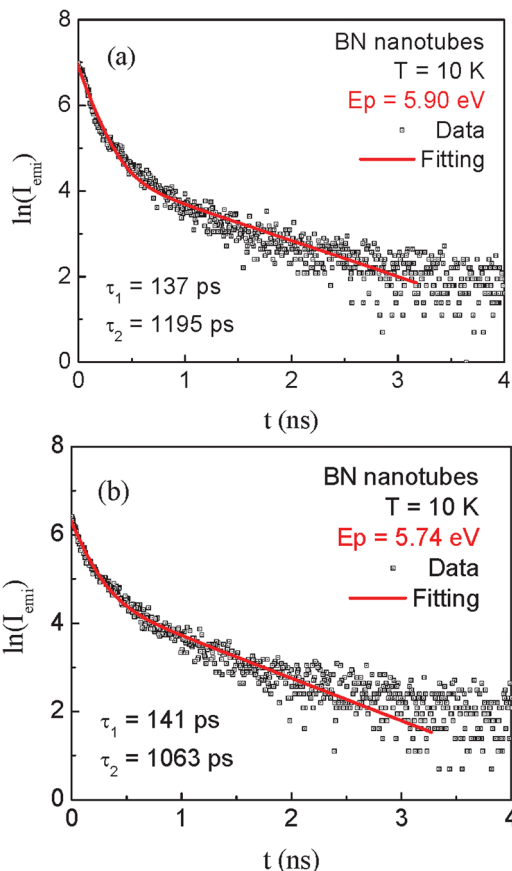


FIG. 3. PL decay kinetics of hBN nanotubes with a diameter of 60 nm measured at emission energies of (a) 5.90 eV and (b) 5.74 eV.

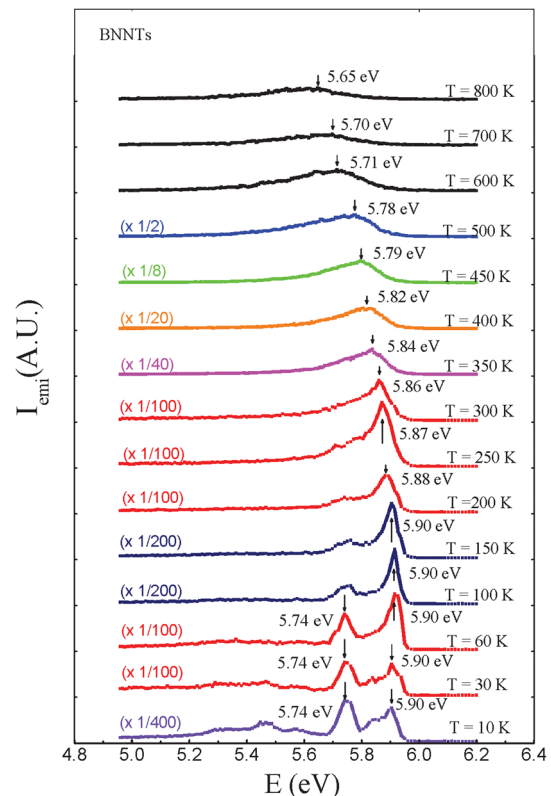


FIG. 4. PL spectra of BNNTs with a diameter of 60 nm measured at a temperature (T) range from 10 K to 800 K.

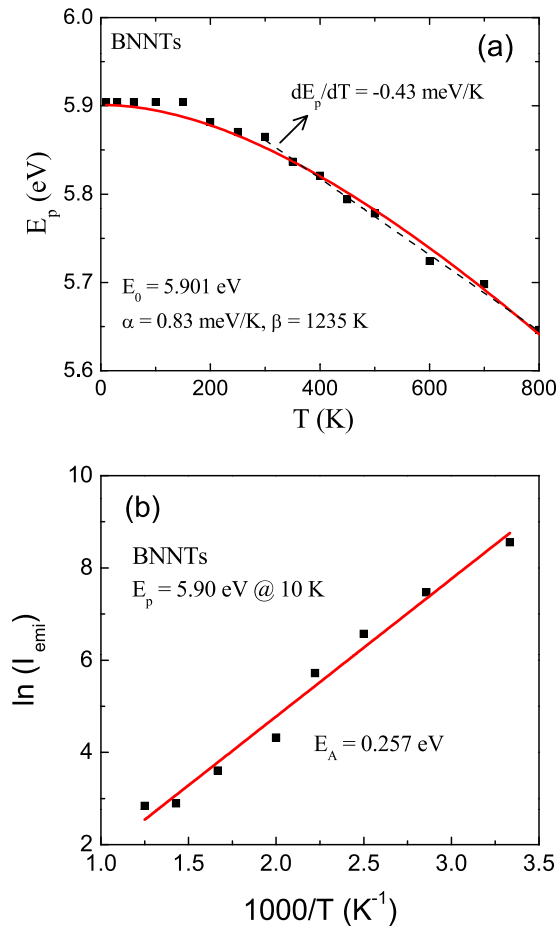


FIG. 5. (a) Temperature dependence of the peak energy (E_p) of the dominant 5.901 eV (at 10 K) emission line in BNNTs with a diameter of 60 nm. The solid curve is the least-squares fit of data with the Varshni empirical equation, $E_p = E_g(T) - (E_X) = [E_g(0) - (E_X)] - \alpha T^2/(\beta + T)$, where the fitted values of α and β are 0.83 meV 0 /K and 1235 K, respectively. The dashed line is the linear fit of data measured at $T > 300$ K with Eq. (2) and the fitted value of $\alpha = 0.43$ meV 0 /K. (b) The Arrhenius plot of PL intensity of the 5.901 eV (at 10 K) emission peak in BNNTs with a diameter of 60 nm.

approximately the Varshni empirical equation describing the temperature dependent bandgap in semiconductors by neglecting the temperature dependence of the exciton binding energy (E_X), $E_p(T) = E_g(T) - (E_X) = [E_g(0) - (E_X)] - \alpha T^2/(\beta + T)$, where $E_g(0)$ is the energy bandgap at 0K, α and β are the Varshni coefficients.²⁸ At high temperatures, the temperature dependence of the excitonic transition peak can be simply written as

$$E_g(T) - (E_X) = [E_g(0) - (E_X)] - \alpha T, \quad (2)$$

where the value of α represents the slope of E_g versus temperature at high temperatures. The slope of E_g versus temperature at high temperatures measured directly from the data between 300 K and 800 K is about 0.43 meV 0 /K. The measured slope of E_g versus temperature is about a factor of 5 times smaller than the theory prediction of ~ 2.1 meV 0 /K for the transitions between the π and π^* bands in 3D hBN.¹⁹ It is also interesting to compare the temperature coefficient of hBN sheets with that of AlN with a comparable energy gap. The measured slope of E_g versus temperature is about 6 times smaller (or equivalently the bandgap of hBN

nanotubes with large diameters or hBN sheets decreases with temperature 6 times slower) compared to a value of 2.4 meV/K for AlN epilayers.²⁹

The temperature coefficients of hBN in 2D or 1D form have not been calculated. However, to the first order, the energy bandgap of hBN single sheets is primarily determined by the energy difference between electron localized on B and N atoms.³⁰ It is reasonable to speculate that the temperature dependence of this energy difference is weaker than those of the energy bandgap of a conventional semiconductor in 3D form. Figure 5(b) shows that the PL intensity also decreases with temperature increasing. An activation energy of 257 meV can be extracted from the temperature dependence of the PL emission intensity. However, the physical origin of this activation behavior is not clear at this stage.

IV. CONCLUSION

In summary, hBN nanotubes with a large diameter (~ 60 nm) have been synthesized and utilized to probe the fundamental optical transitions and the temperature dependence of the energy bandgap of 2D hBN sheets. Due to the combination of the reduced dimensionality effects on the quasi-particle energy gap as well as on the exciton binding energy, the excitonic transition peak was blue shifted by an amount of about 130 meV with respect to that in hBN bulk crystals. Furthermore, due to the absence of the D-series emission lines, the hBN nanotube material system also provides the opportunity to monitor the temperature dependencies of the band edge transitions and of the bandgap of the 2D hBN sheets. The temperature evolution of the excitonic transition line has been probed and revealed that the bandgap energy of hBN nanotubes with large diameters (or equivalently of hBN sheets) decreases with an increase in temperature with a slope of ~ 0.43 meV 0 /K. This temperature coefficient is a factor of about 5 times smaller than the theoretically predicted value for the transitions between the π and π^* bands in 3D hBN and 6 times smaller than the measured value in 3D AlN with a comparable energy bandgap. The observed weaker temperature dependence of the bandgap than those in 3D hBN and AlN is believed to be a consequence of the effects of reduced dimensionality in layer-structured hBN.

ACKNOWLEDGMENTS

The effort on the fundamental optical studies of hBN was supported by DOE (#FG02-09ER46552) and the hBN growth was supported by DHS managed by Dr. Mark Wrobel (#2011-DN-077-ARI048-03). C.D.F. was supported by DOE (#DE-SC0005156). Jiang and Lin are grateful to the AT&T Foundation for the support of Ed Whitacre and Linda Whitacre endowed chairs.

¹B. Arnaud, S. Lebègue, P. Rabiller, and M. Alouani, *Phys. Rev. Lett.* **96**, 026402 (2006).

²B. Arnaud, S. Lebègue, P. Rabiller, and M. Alouani, *Phys. Rev. Lett.* **100**, 189702 (2008).

³L. Wirtz, A. Marini, and A. Rubio, *Phys. Rev. Lett.* **96**, 126104 (2006).

- ⁴Y. Kubota, K. Watanabe, O. Tsuda, and T. Taniguchi, *Science* **317**, 932 (2007).
- ⁵B. Huang, X. K. Cao, H. X. Jiang, J. Y. Lin, and S. H. Wei, *Phys. Rev. B* **86**, 155202 (2012).
- ⁶J. Li, R. Dahal, S. Majety, J. Y. Lin, and H. X. Jiang, *Nucl. Instrum. Methods Phys. Res. A* **654**, 417 (2011).
- ⁷A. K. Geim and I. V. Grigorieva, *Nature* **499**, 419 (2013).
- ⁸T. P. Kaloni, Y. C. Cheng, and U. Schwingenschlögl, *J. Mater. Chem.* **22**, 919 (2012).
- ⁹T. P. Kaloni, M. Tahir, and U. Schwingenschlögl, *Sci. Rep.* **3**, 3192 (2013).
- ¹⁰K. Watanabe, T. Taniguchi, and H. Kanda, *Nat. Photonics* **3**, 591 (2009).
- ¹¹R. Dahal, J. Li, S. Majety, B. N. Pantha, X. K. Cao, J. Y. Lin, and H. X. Jiang, *Appl. Phys. Lett.* **98**, 211110 (2011).
- ¹²S. Majety, X. K. Cao, J. Li, R. Dahal, J. Y. Lin, and H. X. Jiang, *Appl. Phys. Lett.* **101**, 051110 (2012).
- ¹³S. Majety, J. Li, X. K. Cao, R. Dahal, B. N. Pantha, J. Y. Lin, and H. X. Jiang, *Appl. Phys. Lett.* **100**, 061121 (2012).
- ¹⁴J. Li, S. Majety, R. Dahal, W. P. Zhao, J. Y. Lin, and H. X. Jiang, *Appl. Phys. Lett.* **101**, 171112 (2012).
- ¹⁵T. Sugino, K. Tanioka, S. Kawasaki, and J. Shirafuji, *Jpn. Appl. Phys., Part 2* **36**, L463 (1997).
- ¹⁶K. Watanabe and T. Tanniguchi, *Phys. Rev. B* **79**, 193104 (2009).
- ¹⁷K. Watanabe and T. Taniguchi, *Int. J. Appl. Ceram. Technol.* **8**, 977 (2011).
- ¹⁸X. K. Cao, B. Clubine, J. H. Edgar, J. Y. Lin, and H. X. Jiang, *Appl. Phys. Lett.* **103**, 191106 (2013).
- ¹⁹A. Zunger, A. Katzir, and A. Halperin, *Phys. Rev. B* **13**, 5560 (1976).
- ²⁰T. B. Hoffman, B. Clubine, Y. Zhang, K. Snow, and J. H. Edgar, "Optimization of Ni-Cr flux growth for hexagonal boron nitride single crystals," *J. Cryst. Growth* (in press, 2013).
- ²¹P. Jaffrennou, J. Barjon, J.-S. Lauret, B. Attal-Trétout, F. Ducastelle, and A. Loiseau, *J. Appl. Phys.* **102**, 116102 (2007).
- ²²J. Wu, W.-Q. Han, W. Walukiewicz, J. W. Ager III, W. Shan, E. E. Haller, and A. Zettl, *Nano Lett.* **4**, 647 (2004).
- ²³L. H. Li, Y. Chen, M. Y. Lin, A. M. Glushenkov, B. M. Cheng, and J. Yu, *Appl. Phys. Lett.* **97**, 141104 (2010).
- ²⁴L. H. Li, Y. Chen, B. M. Cheng, M. Y. Lin, S. L. Chou, and Y. C. Peng, *Appl. Phys. Lett.* **100**, 261108 (2012).
- ²⁵C. Guo, L. Dong, S. Gong, C. Miao, and X. Zhang, *Appl. Mech. Mater.* **274**, 411 (2013).
- ²⁶J. Serrano, A. Bosak, R. Arenal, M. Krisch, K. Watanabe, T. Taniguchi, H. Kanda, A. Rubio, and L. Wirtz, *Phys. Rev. Lett.* **98**, 095503 (2007).
- ²⁷L. Wirtz and A. Rubio, *IEEE Trans. Nanotechnol.* **2**, 341 (2003).
- ²⁸Y. P. Varshni, *Physica* **34**, 149 (1967).
- ²⁹K. B. Nam, J. Li, J. Y. Lin, and H. X. Jiang, *Appl. Phys. Lett.* **85**, 3489 (2004).
- ³⁰G. W. Semenoff, *Phys. Rev. Lett.* **53**, 2449 (1984).